Article

Controlled Release of Enrofloxacin by Vanillin-Crosslinked Chitosan-Polyvinyl Alcohol Blends

Ilkay Karakurt[1], Kadir Ozaltin[1], Elif Vargun[1,2], Liliana Kucerova[1], Pavol Suly[1], Evghenii Harea[1,3], Antonín Minařík[1,3], Kateřina Štěpánková[1], Marian Lehocky[1,3] *, Petr Humpolícek[1,3], Alenka Vesel[4], Miran Mozetic[4]

[1] Centre of Polymer Systems, University Institute, Tomas Bata University in Zlin, Trida Tomase Bati 5678, 760 01 Zlin, Czech Republic

[2] Department of Chemistry, Mugla Sitki Kocman University, Kotekli, 48000, Mugla, Turkey

[3] Faculty of Technology, Tomas Bata University in Zlín, Vavreckova 275, 76001 Zlín, Czech Republic

[4] Department of Surface Engineering, Jozef Stefan Institute, Jamova cesta 39, 1000 Ljubljana, Slovenia

ykarakurt@utb.cz (I.K.); ozaltin@utb.cz (K.O.); vargun@utb.cz (E.V.); l7_kucerova@utb.cz (L.K); suly@utb.cz (P.S); harea@utb.cz (E.H); minarik@utb.cz (A.M.); k1_stepankova@utb.cz (K.Š); humpolicek@utb.cz (P.H); alenka.vesel@ijs.si (A.V); miran.mozetic@ijs.si (M.M)

***** Correspondence: lehocky@post.cz; Tel.: +420-608-616-048

Received: date; Accepted: date; Published: date

Abstract: In transdermal drug delivery applications uniform drug distribution and sustained release are of great importance to decrease the side effects. In this direction in the present research, vanillin crosslinked chitosan (CS) and polyvinyl alcohol (PVA) blend based matrix-type transdermal system was prepared by casting and drying of aqueous solutions for local delivery of enrofloxacin (ENR) drug. Subsequently, the properties including the morphology, chemical structure, thermal behavior, tensile strength, crosslinking degree, weight uniformity, thickness, swelling and drug release of the CS-PVA blend films before and after crosslinking were characterized. *In vitro* drug release profiles showed the sustained release of ENR by the incorporation of vanillin as a crosslinker into the CS-PVA polymer matrix. Furthermore, the release kinetic profiles revealed that the followed mechanism for all samples was Higuchi and the increase of vanillin concentration in the blend films resulted in the change of diffusion mechanism from anomalous transport to Fickian diffusion. Overall, the obtained results suggest that the investigated vanillin crosslinked CS-PVA matrix-type films are potential candidates for transdermal drug delivery system.

Keywords: Chitosan, Vanillin, Crosslinking, Solvent casting, Drug-polymer solubility, Controlled drug release, Transdermal delivery

1. Introduction

Among several routes of drug delivery applications, the transdermal system has accepted as potential non-invasive routes of drug administration due to its attractive advantages. The main advantages of this non-conventional drug delivery system include the possibility of pain-free therapy, prevention of the pre-systemic metabolism, targeted delivery, providing constant blood levels and avoidance of first-pass metabolism [1,2]. Transdermal systems have designed to deliver the active substances into the systemic circulation via the dermal route in a controlled manner [3]. In such delivery systems, controlled drug release allows distribution of the active substances at a predetermined rate locally or for over an extended period which is significant to ensure a therapeutic concentration in the bloodstream [4,5]. In the case of the doses above this therapeutic index, drugs elicit toxicity against patients and below the

appropriate amount, desired therapeutic effect would not be achieved [6]. Together with the controlled release characteristics, transdermal delivery also ensures the protection of the pharmacological properties of the drug when loaded in a polymer matrix [7].

In recent years, substantial research has been reported to produce a biopolymer-based potential transdermal delivery device for effective transportation of drug molecules across the skin [8]. However, the skin acts as a primary barrier for drug penetration due to the presence of hydrophobic lipid membrane on the outermost layer (stratum corneum) [9]. This layer consists of dead keratin filled cells (ie. corneocytes) which are surrounded by continuous lipid bilayers [10]. In order to reach systemic circulation via penetration, an active substance has possible pathways according to the lipid-protein-partitioning theory [11]. As shown in Figure 1, in the intercellular route drug molecules are transferred around the corneocytes while in the intracellular way delivery into the bloodstream occurs passing through the cell membrane. Regarding a variety of approaches, to be able to deliver the active substances into the systemic circulation, polymeric materials are widely studied due to their remarkable effect on local skin penetration.

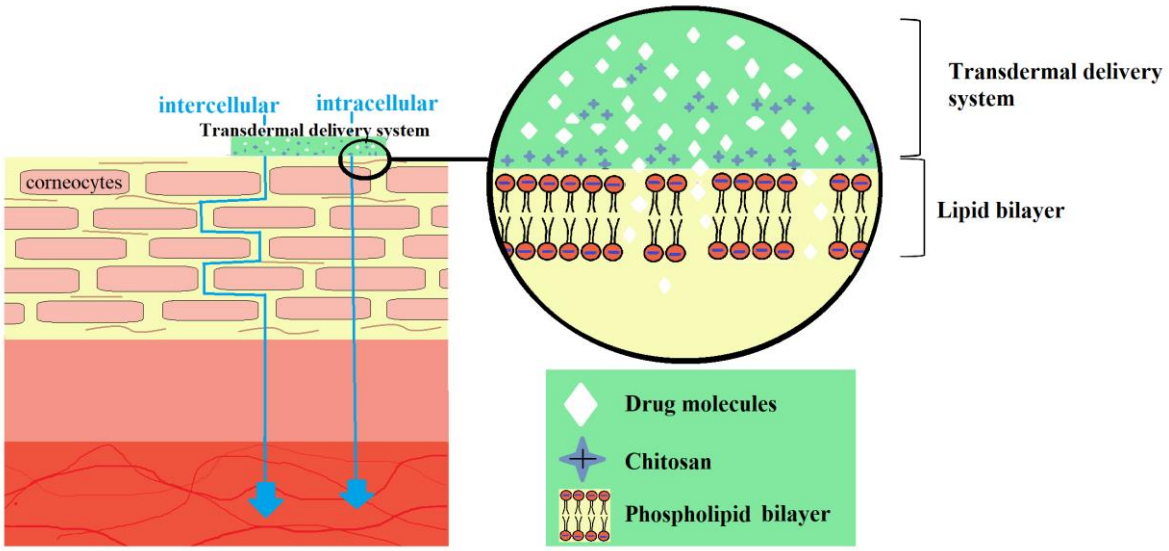

Figure 1. Pathways of permeation through skin and the permeation-enhancing effect of CS

Transdermal drug delivery devices originated from synthetic or natural or both polymers typically provide the necessary structural support for diffusion and drug administration through skin. Plenty of works report on the literature potential transdermal patches fabricated from several polymers (pure or blend) using different processing techniques such as hydrogels, microspheres, nanoparticles and nanofibers [12]. Among these, preparing polymer films by solvent casting technique has been favorably applied due to easy processing, reproducibility, cost-effective production and stability properties [13]. In this regard, polysaccharides are a prominent class of biopolymers used to design matrix-type systems for transdermal delivery applications with controllable chemical and mechanical properties [14].

Chitosan (CS), a derivative of the biopolymer chitin, has been widely processed in the biomedical field as a good film-forming matrix [15]. Besides wound healing and tissue engineering applications, CS shows promising features to be used as an auxiliary agent in drug delivery systems owing to its unique properties, including biodegradability, biocompatibility, permeation enhancement, hemostatic capability, bactericidal and fungicidal activity [16-18]. These properties are closely related to the molecular weight as well as the primary amino groups of CS which make it a unique biomaterial among all the other biodegradable polymers by exhibiting a cationic character [19]. So this positively charged linear structure enables the interaction with the negatively charged phospholipid and reversibly alters the physicochemical nature in lipid bilayer of the stratum corneum to enhance the drug diffusion into

deeper layer of skin [20]. Moreover, it is known that modification of these amino and hydroxyl groups on the CS structure could impart improved properties and particular biological functions such as solubility, mucoadhesion, and bio-adhesivity [21]. There are several ways can be used to alter the CS backbone with the purpose of tailoring the network structure of the polysaccharide to suit specific applications.

Crosslinking is a well-known and proven technique to modify the CS backbone and to reduce segment mobility in the polymer chains causing a three-dimensional network structure [22]. Crosslinking affects the hydrophilicity, swelling behavior, biodegradation rate, stability, dispersivity, controlled release, drug targeting and mechanical properties [23-25]. Some of the crosslinkers to improve these properties are glutaraldehyde, formaldehyde, tripolyphosphate and glyoxal [26,27]. However, these agents present several problems related to their potential side effects and environmental impact which limit their usage as crosslinkers in pharmacological applications. Within this context, more attention has been paid on green and natural crosslinking agents, such as plant extracts (polyphenols and aldehyde compounds) [28].

Vanillin, which exists in seedpods of vanilla (*Vanilla planifolia*), is one of the most prevalent additives and widely used as a flavoring and preservative agent in practical applications such as food, beverages, perfumery and pharmaceutical industry [29-31]. It is a significant bio-based monomer and exhibits bioactive properties such as antitumor, anti-inflammatory, antioxidant and antimutagenic activities [32,33]. The aldehyde group of vanillin, which leads to identifying it as a natural crosslinker, constitutes a Schiff-base bond with the amino groups of CS, and also the hydroxyl group of this crosslinker can form a hydrogen bond with the amino or hydroxyl groups of another CS molecule (Figure 2) [31]. With the formation of these hybrid network structure, the molecular mobility of the drug molecules in the CS polymer matrix is restricted and the stability, dispersivity as well as the release control of the drug are improved in the local delivery system [34,35].

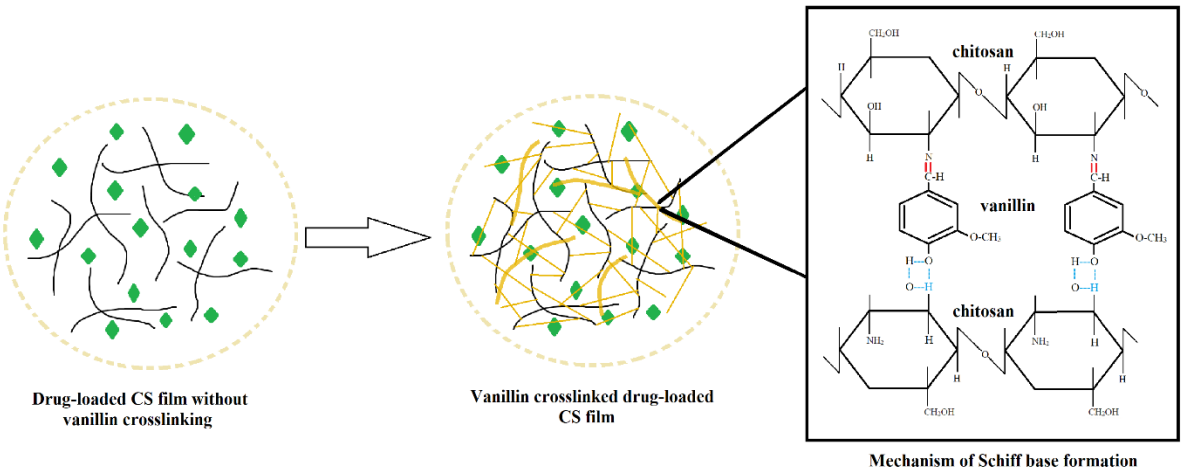

Figure 2. Schematic representation of Schiff base formation between CS and vanillin

However, the natural brittleness of most of the polysaccharide-based films (i.e. CS) limits their applications, and to overcome this limitation using a biocompatible and non-antigenic copolymer, like PVA, to be blended with CS can be an effective strategy. The proper amount of PVA contributes to improve the flexibility and the elongation of the CS films and eliminate the necessity to use plasticizers [36].

So far, the crosslinking of CS with vanillin for the drug delivery purpose investigated in the literature. Although considerable attempts devoted to improving the sustained release of several drugs incorporated into vanillin crosslinked CS microspheres [37] and nanoparticles [32,38], less attention has been paid to vanillin crosslinked films to improve drug-polymer solubility and controlled release.

Drug-polymer solubility may represent the essential parameter for the uniform distribution and sustained release of drugs [39]. Insufficient drug-polymer solubility may lead to drug nucleation of crystalline form and accelerate the crystal growth [40]. For drug release applications, this behavior may ultimately result in reduced product performance, physical stability issues, and lower bioavailability which will neutralize the advantages of transdermal delivery systems [41,42]. One way of enhancing drug-polymer solubility of poorly soluble drugs in the solid dispersions is the restriction of molecular mobility, thus preventing uncontrolled drug recrystallization [43]. In this study, vanillin used as a crosslinker to create a network structure that can limit the segment mobility with the aim of homogenous drug dispersivity and controlled release.

Overall, the main aim of this study is to prepare polymer blend films using high molecular weight-CS and PVA (CS-PVA) and to evaluate the efficacy of vanillin as a crosslinking agent on drug release studies. To test the drug release behavior of the films, ENR was used as a poorly-water soluble model drug. Also, this combination in matrix-type transdermal system prepared without using any plasticizer or permeation enhancer was not studied well according to the past literature. The physicochemical and mechanical properties of the prepared films were analyzed by Scanning electron microscopy (SEM), Fourier transform infrared spectroscopy (FTIR), Atomic Force Microscopy (AFM), Laser Scanning Confocal Microscope (LSCM), X-ray photoelectron spectroscopy (XPS) and Thermal gravimetric analysis (TGA). Furthermore, the degree of crosslinking, swelling properties and the release kinetics of the polymer blends were also investigated by the ninhydrin assay, measuring mass change in dry-swollen states of films, and 'sample and separate *in vitro* method', respectively. The possible outcomes from the study revealed that vanillin crosslinked CS-PVA blend films can sustainably release and stabilize ENR so as to achieve better therapeutic efficacy which show promising potential to perform as transdermal drug delivery systems.

2. Materials and Methods

2.1. Materials

High molecular weight CS (310-375 kDa) with 75-85% degree of deacetylation, vanillin (99%) and ninhydrin were purchased from Sigma Aldrich (Prague, Czech Republic). Acetic acid (99.8%) was supplied from Microchem (Pezinok, Slovakia), ENR (Mw 395 Da) and PVA 8-88 (Mw ~ 67,000, degree of hydrolysis 86.7–88.7 mol%) were obtained from Fluka Bio-Chemika (Steinheim, Germany). Ethanol (99.8%, spectral) was obtained from Riedel-de Haën (Seelze, Germany), and phosphate-buffered saline was obtained from Biosera (Prague, Czech Republic). All the reagents were analytical grade.

2.2. Preparation of Polymer Films

The high molecular weight CS solution with a concentration of 1%(w/v) was prepared by dissolving CS in aqueous acetic acid solution (2% v/v) under magnetic stirring at 50 ºC for 2h until its complete dissolution. Then the crosslinking agent solutions were prepared by dissolving vanillin at different concentrations (1% and 3% w/v) in ethanol. Next, CS and vanillin solutions were mixed and the mixture was stirred continuously at 50 ºC for crosslinking reaction. ENR was loaded to the film preparation in a concentration of 1%(w/v). Thereafter, PVA dissolved in distilled water (1% w/v) was poured into all sample solutions to solidify the biopolymer films with the final ratio of PVA and CS at 1:2 (w/w). Finally, the film solutions were poured into polytetrafluoroethylene Petri dishes (8×8cm) and subsequently allowed to dry at room temperature for 24h. The peeled films obtained were stored in airtight containers at room temperature before further testing. All the film preparation steps are graphically presented in Figure 3.

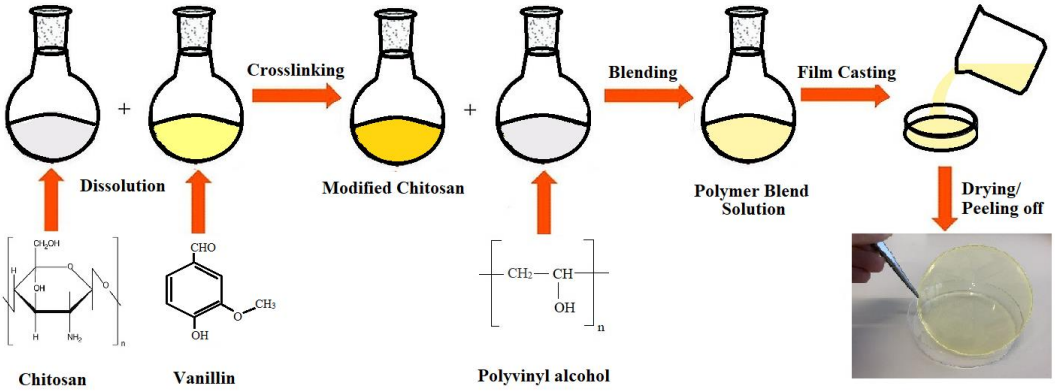

Figure 3. The scheme of vanillin crosslinked CS-PVA film preparation with solvent-casting method

2.3. Analytical Methods

The surface structure of the polymer blend films was observed using a NANOSEM 450 (FEI, Hillsboro, OR, USA) scanning electron microscope at 5.0 kV of accelerating voltage after sputter coated with conductive gold/palladium layer.

The surface roughness and topology at nanometer scale of the drug loaded blend films were measured with an AFM (Dimension Icon Bruker, Karlsruhe, Germany) in peak force tapping mode (noncontact mode) using a ScanAsyst-Air Si/Nitride probe (Bruker, Santa Barbara, CA, USA) with k = 0.4 N/m of spring constant value of the cantilever. Data were acquired on a scanning area of 5.0 × 5.0 µm for each sample with a scan rate of 1 Hz. Images were processed using the Gwyddion – Free SPM data analysis software, version 2.55 (Czech Metrology Institute, Czech Republic) The height profiles and surface roughness (*Sa*) were determined.

The appearance, thickness and mass uniformity were examined for visual evaluation of the polymer films. The film thickness was measured at three random positions on the film by a digital micrometer having a sensitivity of 0.001 mm. For the mass uniformity assessment, the films from casting plates were cut into 2.5 × 2.5 cm square shapes (triplicate) and weighted by using a digital scaler.

The functional group identification in the blend films were examined by means of Fourier Transform Infrared Spectroscopy (Nicolet iS5, Thermo Fisher, Waltham, USA). All ATR-FTIR spectra were obtained at 64 scans at a resolution of 4 cm^{-1} over a wavenumber range of 4000-600 $cm^{-1.}$ All the readings performed at room temperature (25 ± 1ºC). The processing of the spectra was achieved using the Origin Pro program.

The elemental analysis of non-crosslinked and vanillin crosslinked CS-PVA blend films were investigated with X-ray photoelectron spectroscopy (XPS) using the TFA XPS Physical Electronics (Munich, Germany). Samples were placed on the sample holder and the base pressure in the analysis chamber was set to 6×10^{-8} Pa. As the photoemission excitation, a monochromic Al $K\alpha_{1,2}$ X-ray source (1486.6 eV) line was applied on the three different place on each sample with a 400µm spot size. Photoelectrons were detected with a hemispherical analyzer, mounted at an angle of 45° and the energy resolution was about 0.6 eV. Surface elemental concentrations were calculated from survey-scan spectra which were aligned by setting the C1s peak at 285.0 eV, using the Multipak software version 9.6.0.

The distribution of ENR in blend films was studied by Laser Scanning Confocal Microscope (LSCM) Olympus FLUOVIEW FV3000. Excitation wavelengths were 405 and 561 nm. The emission detection window for the identification of ENR was set to 430-470 nm based on the data in the literature [44]. The objective with magnification 60x was used for analysis.

Thermal analysis was carried out using a TGA Q500 (TA Instruments, USA) thermogravimeter under a nitrogen atmosphere with a flow of 50 mL min^{-1}. The temperature range of 25-600 ºC was tested for thermal stability at a heating rate of 10 ºC min^{-1}. The Universal Analysis 2000 system was used for the evaluation of the data.

The mechanical properties of the films were determined with a Testometric M350 tensile machine (Testometric Company, Ltd. UK) according to the methodology described in Reference [44]. The films were conditioned at room temperature, 50% relative humidity (RH) for 48 h and cut into strips (80 mm×10 mm) prior to analysis. The test was performed at a crosshead speed of 5 mm/min with the initial grip separation of 40mm. Five specimens were tested for each sample and the average value was calculated. The tensile properties (Young's modulus, elongation at break, and tensile strength) were evaluated by stress-strain curves.

The crosslinking degree of blend films was evaluated by ninhydrin assay [45] with quantitatively determination of the ratio of consumed amino groups by reacting with vanillin to the free amino groups in the non-crosslinked films. For the ninhydrin reagent preparation, Solution A (1.05 g citric acid, 0.4g NaOH and 0.04 g $SnCl{\cdot}H_2O$ were dissolved in 25 mL deionized water) and Solution B (1 g ninhydrin in 25 mL ethylene glycol monomethyl ether) were mixed and stirred for 45 min, then stored in the dark bottle until further usage. The test samples were weighed and heated with 2 ml ninhydrin reagent at 100°C in a water bath for 30 min. After cooling down to room temperature, the solutions were diluted with 1ml of 50% ethanol and subsequently the optical absorbance at 570 nm was recorded with an UV spectrophotometer (Xylem Analytics Germany Sales GmbH & Co. KG, Weilheim, Germany). The cross-linking degree of samples are calculated as follows:

$$\text{Crosslinking degree (\%)} = \frac{Co - Cv}{Co} x100\ \% \qquad (1)$$

where Co is the concentration of free amino groups in non-crosslinked samples and Cv is concentration of free amino groups remaining in crosslinked samples. The experiment was repeated three times for each sample and the result was expressed as an average value.

2.4. Swelling Measurement

The gravimetric method was performed to evaluate the swelling behavior of the blend films as a function of the percentage of vanillin incorporated into the film formulations. For this, the films (triplicate) without drug were dried to a constant weight and cut into 2.5 × 2.5 cm square shapes. Then pre-weighed samples were immersed into a beaker containing 20 mL phosphate buffer solution (PBS) (0.1 M, pH 7.4) and kept under constant slow stirring at room temperature for 24h. At each specified time point, the films were taken from the solution and the excess surface water was removed gently by blotting filter paper. Subsequently, the swollen films were weighed and the swelling degree was calculated using equation [23]:

$$\text{Swelling Degree (\%)} = \frac{Ws - Wi}{Ws} x100\ \% \qquad (2)$$

where (*Wi*) is the initial weight and (Ws) is the weight of the sample in the swollen state.

2.5. In-vitro Drug Release Test

The *in vitro* drug release study of ENR from non-crosslinked and vanillin crosslinked films was conducted in PBS with pH 7.4 to mimic the *in vivo* environment. Briefly, the films with an area of $4cm^2$ were placed into 10 mL of PBS media and placed on an oscillating stirrer (100 rpm).

At the predetermined time intervals, aliquot samples (1 mL) were withdrawn and replaced with the same volume of fresh media. After the samples appropriately diluted, the drug contents were spectrophotometrically analysed by a Photolab 6600 UV-VIS photometer (Xylem Analytics Germany

Sales GmbH & Co. KG, Weilheim, Germany) at a wavelength of 285 nm for ENR. These studies were performed in triplicates.

Besides, the desorption method was used to estimate the loading capacity of the films. For this, the blend films were introduced in 2% (v/v) acetic acid for 3 days, subsequently the aliquots of the desorbed solutions (1 mL) were withdrawn and their absorbance was measured by UV–VIS spectroscopy to compare with the corresponding calibration curve ($\lambda = 285$ nm, Abs = 0.0814 (ug mL^{-1}); $R^2 = 0.9991$)

2.6. Statistical Analysis

For statistical comparison of data obtained from this study, one-way analysis of variance ANOVA was employed using Microsoft Excel 2016, using ($P < 0.05$) as a significance level.

3. Results and Discussion

3.1. Surface Chemistry and Morphology

The appearance of the ENR loaded CS-PVA blend films is shown in Figure 4. As can be seen, the orange logo on the background can be identified clearly through drug-loaded blend films which confirms the formation of a homogeneous structure. The ENR loaded non-crosslinked film (Figure 4a) is transparent without any color tone, but the vanillin crosslinked films show a yellowish tint, which is attributed to the imine bond formation [46]. It is found that the films containing the low concentration of vanillin have less opacity than those with a higher concentration, which is due to the difference in –NH_2/–CHO molar ratios (1/1 and 1/3) corresponding to the Schiff bases.

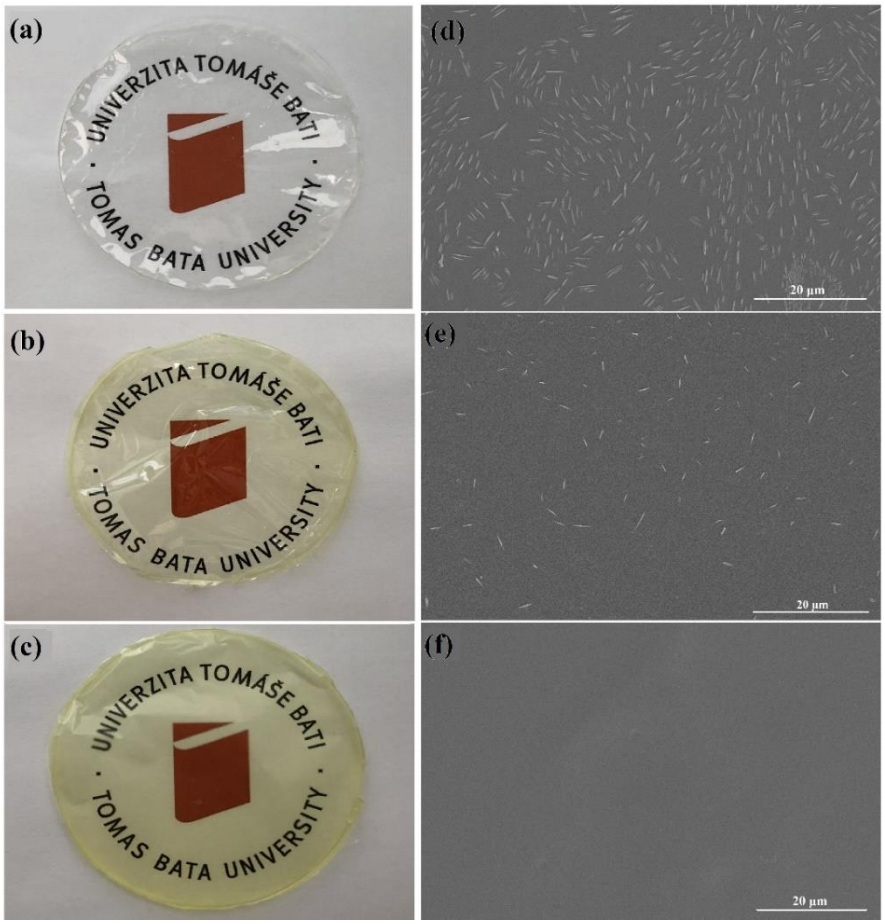

Figure 4. Photographic images and SEM micrographs of (a,d) CS-ENR-PVA; (b,e) CS-1V-ENR-PVA; (c,f) CS-3V-ENR-PVA

Figure 4 also shows the SEM micrographs of the surface of ENR-loaded CS-PVA based films with various concentrations of vanillin. As observed in SEM images, all samples show a plain and dense structure without pores. Furthermore, there can be seen some microcrystal form of ENR molecules randomly distributed over the CS-ENR-PVA non-crosslinked film surface (Figure 4d) which can probably be attributed to the low interactions between the drug and the polymer blends. With the vanillin addition, these microcrystal forms of drug molecules are significantly decreased on the CS-1V-ENR-PVA blend surface (Figure 4e). In case of increase in vanillin concentration from 1% to 3%, those structures become invisible and more uniform surface is observed on the CS-3V-ENR-PVA film micrograph. It is assumed that drug molecules bonded to CS-PVA matrix in the course of crosslinking reaction are not seen in the SEM micrographs due to the uniform distribution in polymer blend matrix. In order to confirm the presence of ENR and the interaction between drug and polymer substrates, FTIR spectrum and XPS were employed as tools for the measurement. It may be concluded from the SEM images that the crosslinking of the polymer blend with vanillin exerted the stabilizing effect of the polymer and minimized the risk of drug agglomeration [34,35]. To further understand the alterations on the drug loaded CS-PVA films AFM was performed.

Table 1 shows the average surface roughness values and cross section profiles of non-crosslinked and crosslinked drug loaded CS-PVA films. The blend film which has the highest surface roughness value of 17.9 is non-crosslinked CS-ENR-PVA. Moreover, irregular particles and macro-agglomerates which may belong to drug particles are observed on the topography image as is observed from the SEM image. However, with 1% vanillin incorporation to the films these cluster structures diminishes and surface roughness drastically reduces to 10.2 nm. Further increase in vanillin concentration up to 3% makes the film homogenous, smoother and these agglomerations become invisible. Similar results have been reported by various researchers in case of other chitosan crosslinking based films and membranes [47,48].

Table 1. Average roughness values and AFM images of drug loaded CS-PVA blends

Sample type	AFM Image	Cross section
CS-ENR-PVA	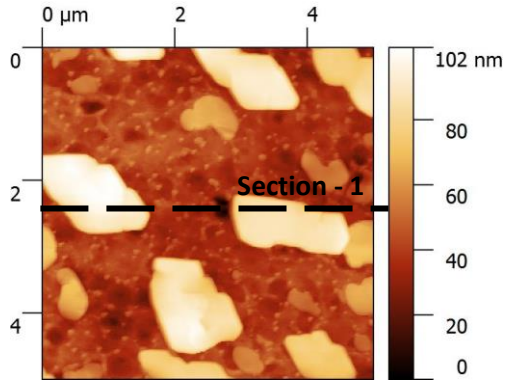	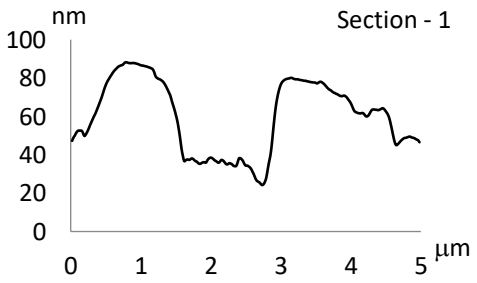 *Sa* = 17.9 nm
CS-1V-ENR-PVA	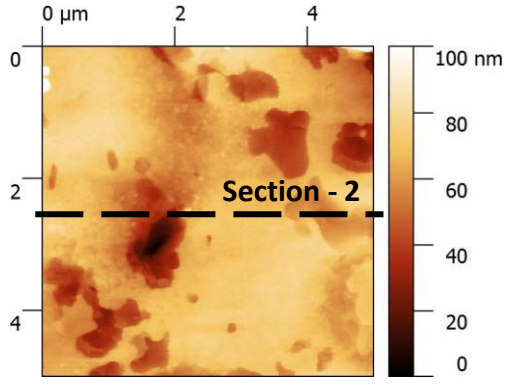	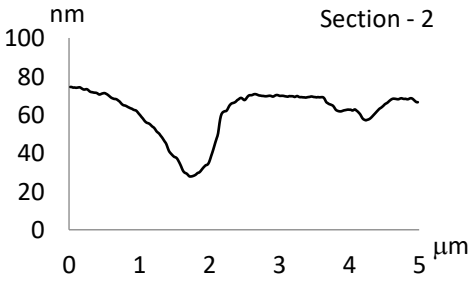 *Sa* = 10.2 nm

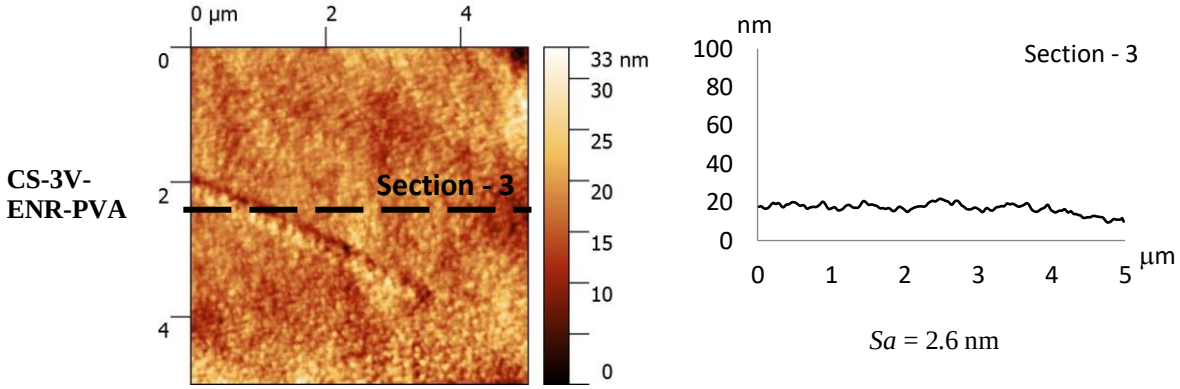

For uniform distribution of drug molecules, weight and thickness parameters are the key variables that control the sustained delivery [49]. The thickness of the films was found to be in the range of 7.2 ± 0.4 µm to 16.7 ± 1.9 µm and the weight of the films (2×2 cm^2) were between 7.0 ± 0.3 mg to 10.6±2.4mg (Table 2). Transdermal films of ENR were found to have uniform thickness and weight which ensured homogeneity.

Table 2. Values for thickness, weight and the swelling index for the prepared films

Sample type	Thickness (µm)	Weight (mg)	Swelling Degree (%)
CS	14.0 ± 0.7	7.0 ±0.3	319.3
CS-PVA	7.2 ± 0.4	7.0 ± 1.4	243.7
CS-1V-PVA	10.8 ± 0.8	7.3 ± 1.5	43.3
CS-3V-PVA	16.7 ± 1.9	10.6 ± 2.4	36.3

The distribution of ENR in polymer blends was studied by LSCM. The typical emission wavelength for ENR is in the range of 450-455 nm [44]. As shown in Figure 5, CS-PVA blend film without ENR gives no fluorescence signal in the range of 430-470 nm. For samples with ENR, fluorescence signals are obtained in the blue to cyan colored images. However, the emission intensity of blue color decreases with the increase of vanillin content. In the drug loaded non-crosslinked sample, the surface is emitting blue without discontinues. This could be attributed to the abundance of microcrystal form of ENR molecules on the film surface, as can be seen in SEM images (Fig 4-d). With the vanillin incorporation, obtained fluorescence signal is decreased and CS-3V-ENR-PVA films exhibits a considerably reduced cyan emission. This might be result of the minimized risk of drug agglomeration on the surface and restricted the molecular mobility of the drug molecules in the hybrid network structure as demonstrated in Figure 2. The XPS results and drug loading tests shows that the highest drug amount detected on CS-3V-ENR-PVA films. In contrast to these results, a reduce in the emission intensity of ENR molecules might be explained by aggregation-induced emission enhancement theory in which the photoluminescence efficiency of luminophores increase by aggregation [51]. To gain further insight into ENR photophysical property, further investigation is needed.

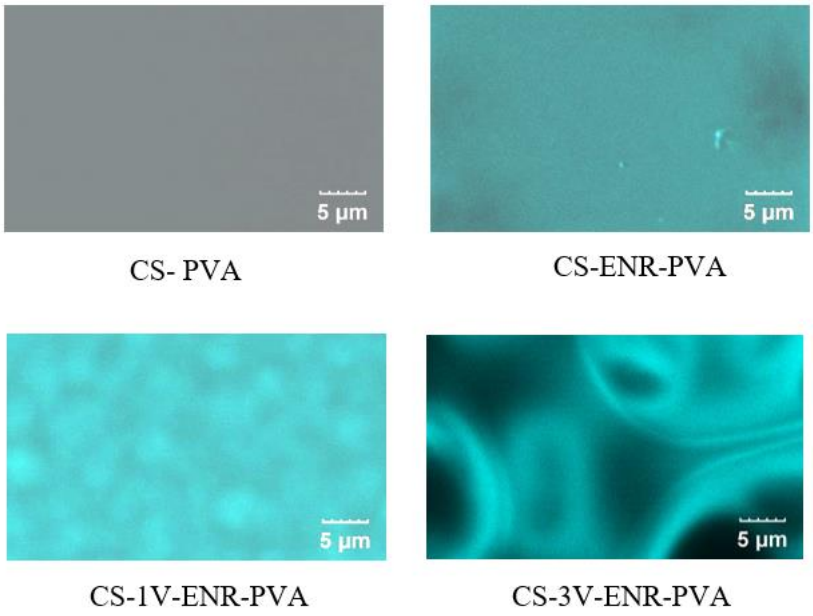

305

306 **Figure 5.** Laser Scanning Confocal Microscope (LSCM) comparison of polymer films at fluorescence signal in
307 the range 430-470 nm

308 The ATR-FTIR spectra of CS-PVA blends with different vanillin content and with/without ENR loaded
309 films are presented in Figure 6. The FTIR spectrum of CS-PVA blend film reveals the characteristic
310 peaks of both CS and PVA (Figure 6a). The –OH stretching of PVA and –NH stretching of CS are
311 overlapped and appeared as a broad band between 3355 cm^{-1} and 3286 cm^{-1}. The asymmetric and
312 symmetric –CH stretching of $–CH_2$ groups of PVA and CS are observed at 2923 cm^{-1} and 2854 cm^{-1},
313 respectively. The peak at 1727 cm^{-1} is attributed to the C=O bond stretching of PVA from the remaining
314 acetate groups during the production of PVA from polyvinyl acetate [52]. The N–H bending in amino
315 ($–NH_2$) groups and O–H bending in hydroxyl groups of CS are clearly identified at 1550 cm^{-1} and 1411
316 cm^{-1}, respectively [53]. The C–H vibrations in the ring are identified as a peak at 1326 cm^{-1} for CS. The
317 peak at 1257 cm^{-1} corresponds to the C–O stretching for PVA. The characteristic C–O–C vibrations in
318 rings of CS are observed as sharp peaks at 1072 cm^{-1} and 1033 cm^{-1} [54].

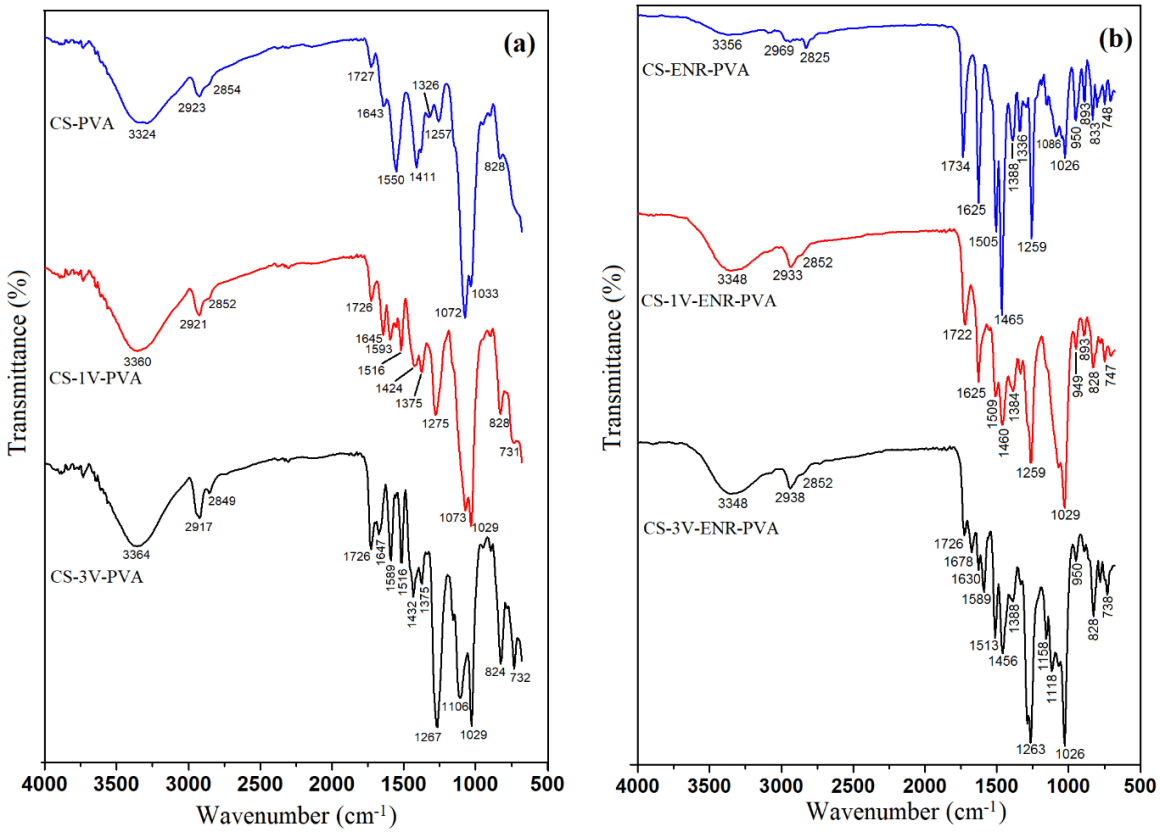

Figure 6. FTIR spectra of (a) without drug loading CS-PVA blends; (b) ENR loaded CS-PVA blends with different vanillin content

The FTIR spectra of crosslinked CS-PVA blends with 1% and 3% vanillin exhibited the major peaks associated with CS and PVA components. For 1% vanillin crosslinked blend film (CS-1V-PVA) exhibited some differences from the non-crosslinked one. The OH band at 3324 cm^{-1} shifted to the 3360cm^{-1} that indicating the generation of the hydrogen bonding between CS and vanillin [37]. The peak at 1645 cm^{-1} can be seen clearly due to the stretching vibration of the C=N bond that confirms the crosslinking reaction between the NH_2 group of CS and the HC=O group of vanillin [55]. Besides, the C-C stretching of vanillin ring can be identified at 1593 cm^{-1} and 1516 cm^{-1}. The peak at 1275 cm^{-1} shows the ether groups (-C-OCH_3) in vanillin [56]. The FTIR spectrum of CS-PVA blend showed the vanillin related peaks more distinguished when the three times higher vanillin content was used (CS-3V-PVA). The peak intensities at 1589 cm^{-1} and 1519 cm^{-1} of the benzene ring of vanillin increased significantly. The vanillin rings out of plane bending vibrations become clear at 732 cm^{-1} [57]. The three times increment of the vanillin content did not change the OH band related to the hydrogen bonding.

ENR originated FTIR absorptions can be clearly identified in the spectrum of ENR loaded CS-PVA blends (Figure 6b). The sharp peak at 1734 cm^{-1} is due to the C=O vibration of both ENR and PVA. Also, the C=O stretching absorption peak of ENR ring is observed at 1625 cm^{-1} [53]. The C=C stretching vibrations of the aromatic ring and C-F bonds of ENR are appeared at 1465 cm^{-1} and 1259 cm^{-1}, respectively [58]. The increased vanillin content in the formulation was also confirmed by the FTIR analysis. The typical C=C stretching of the vanillin ring and out of plane bending vibrations of vanillin ring at 1589 cm^{-1} and 738 cm^{-1} can be identified respectively. Moreover, the spectrum of 3% vanillin crosslinked ENR loaded film also confirmed that there is an interaction between the ENR and CS-PVA blends. After the drug loading, the shifting of the peaks of –OH stretching and carbonyl peaks became clear and this drug-matrix interaction might be due to the polar functional groups in ENR [59].

The quantitative atomic compositions of the CS-PVA blend films was determined by XPS measurements. The elemental content of carbon, oxygen, nitrogen, and fluorine in each sample is shown in Table 3. According to the chemical structure of CS and PVA, the XPS analysis of the blend films

without drug content indicates that the surface is dominated by carbon and oxygen species. Small amounts of nitrogen were also detected which assigned to CS backbone.

Table 3. The atomic weight percentage of CS-PVA blend films

Sample type	Composition (%)				Ratio
	C	N	O	F	O/C
CS-PVA	71.7	5.1	23.2	-	0.32
CS-1V-PVA	72.4	4.1	23.5	-	0.33
CS-3V-PVA	71.1	4.1	24.8	-	0.35
CS-ENR-PVA	67.5	6.4	25.4	0.6	0.38
CS-1V-ENR-PVA	72.8	5.6	20.9	0.8	0.29
CS-3V-ENR-PVA	74.4	2.9	21.6	1.1	0.29

As it is shown in Table 3, antibiotic drug-loaded films display fluorine concentrations between 0.6-1.1% due to the incorporation of the ENR. In accordance with the structure of ENR that contains only one fluorine atom, these low concentrations were expected. Nitrogen is present as well in ENR, however, its concentration is lower than in CS. The concentration of nitrogen decreases from 6.4% to 2.9%, while fluorine shows the opposite trend by increasing the vanillin content. The presence of fluorine (C-F bond) can be also observed in carbon spectrum as a new peak at about ~289 eV (Figure 7), which allows determining the highest drug content of the films. The highest drug amount detected on CS-3V-ENR-PVA films may be due to the increased crosslinking degree introduced by vanillin addition, leading to more widespread immobilization of the drug. When the results are evaluated together with the SEM images given in Figure 4, it is seen that vanillin leads to an improvement in the stabilizing effect of the polymer which results in better interactions with drug molecules.

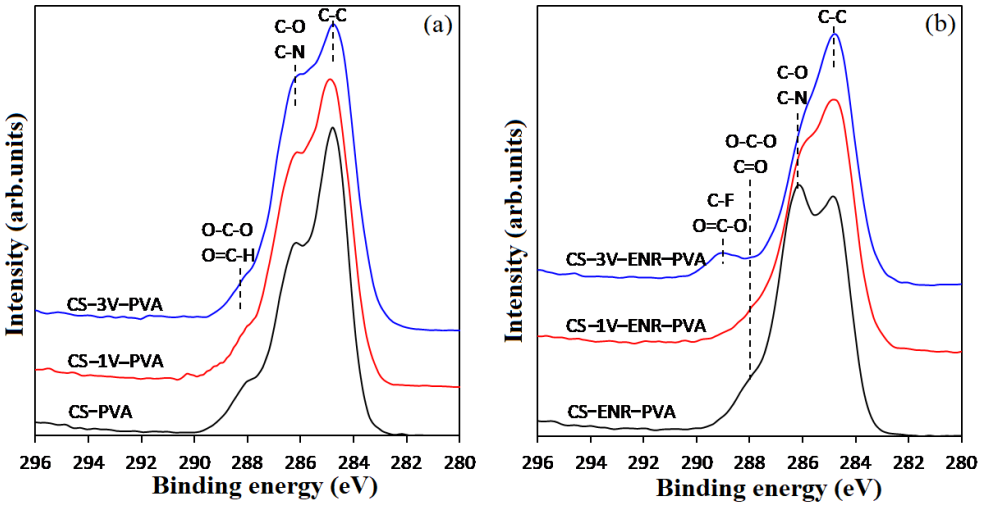

Figure 7. High-resolution XPS spectra of carbon C1s peak.

The thermal behavior of the raw films (CS, PVA) and the blends with different vanillin concentration was investigated by TGA-DTG analysis (Figure 8). It can be seen from the TGA curves all films show weight loss in a range of 4-11% at 30-130 °C due to the moisture and volatile compounds evolution. CS film shows the thermal degradation at 295 °C whereas PVA film thermogram exhibits two onsets regarding its hydroxyl side groups degradation at 316 °C and polyene backbone degradation at 447 °C [60] (Figure 8a). The TGA trend recorded for the CS-PVA blend is similar to those of raw CS and PVA films. However, TGA curves of CS film shift toward high temperature (to 301 °C) along with the PVA content, which confirms an increase in the thermal stability of the blend film regarding only CS film. Also, the DTG peak for CS-PVA blend at the 162 °C (Figure 8b) accounts for acetic acid and water interaction with polar domains [61] which led to a broad and shifted peak. On the other hand, the addition of vanillin slightly decreases the thermal stability of the CS-PVA matrix to 291 °C when the amount of vanillin is equal or higher than 1 wt.% (Figure 8d). In accordance with this finding, Abraham

et al. [21] and Kasai et al. [33] studied the effects of vanillin and PVA on thermal properties of CS films and found that thermal stability of CS matrix with PVA slightly decreased by vanillin content. However, the obtained higher initial decomposition temperature (290 °C) confirms that the drug-loaded polymer blends with vanillin are highly thermally stable.

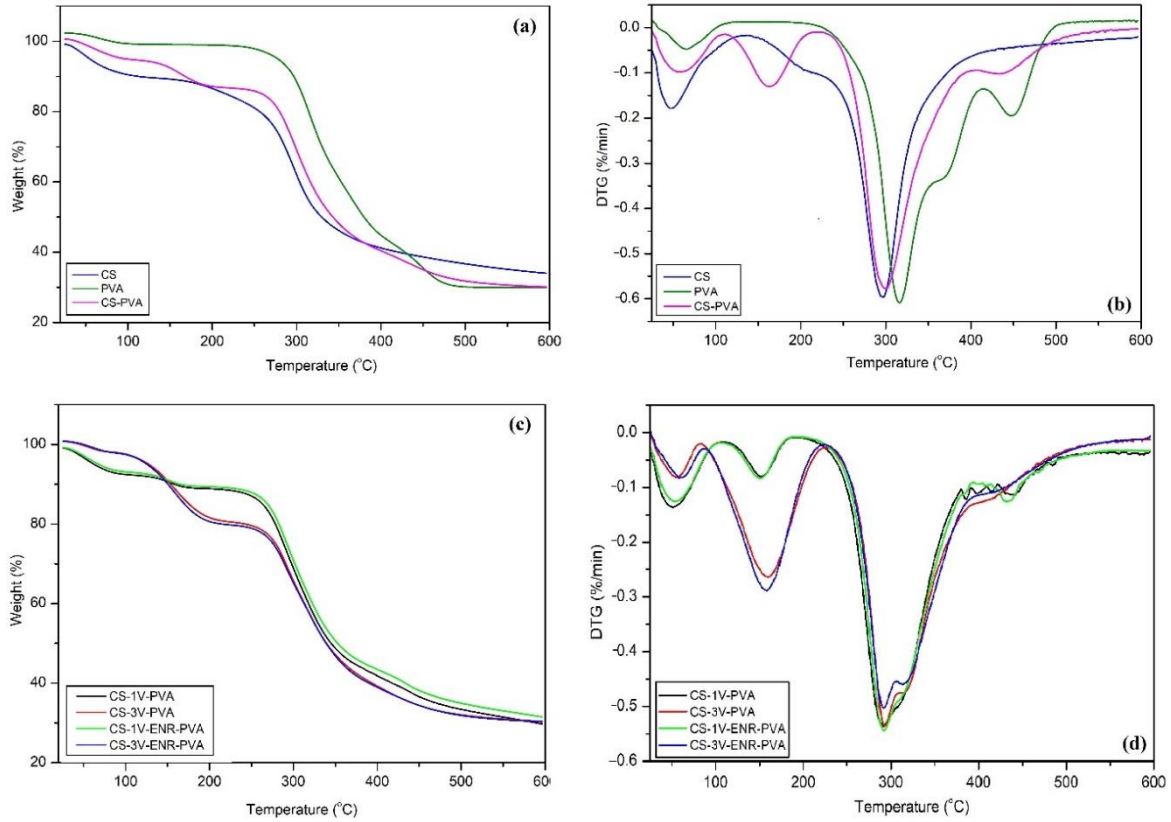

Figure 8. TGA (a,c) and DTG (b,d) curves for CS, PVA, and blend films with different vanillin content.

The mechanical performance of CS-PVA blend films and the effects of vanillin content were investigated based on tensile strength (TS), elongation at break (EB), and young modulus (YM). As it is shown in Table 4, CS-PVA films exhibit the lowest TS and YM values, and with the addition of vanillin, the mechanical properties of CS-1V-PVA films increased by 18.9%. However, EB of vanillin crosslinked films slightly decreased from 1.65% to 1.53% when compared to non-crosslinked films. By further increasing the vanillin content in the blend matrix, TS continue to rise and YM has reached to a maximum value of 5.16 GPa, meanwhile EB decreases to a lowest value of 1.47%. These improvements may ascribe to the crosslinking reaction between functional groups of CS and vanillin in which the mobility of polymer chains is restricted and thereby the rigidity is augmented [62,63]. In the literature, it is stated that increasing amount of crosslinking agents leads promoted TS and decreased EB of biopolymer films [63]. A similar study on ethyl vanillin crosslinked CS-PVA based composite films prepared by Narasagoudr et al. [64] reported an almost 2-fold increase in TS, and in other study Zhang et al. [26] stated that vanillin incorporation led to a 1.53 fold increment in the mechanical properties.

Table 4. Tensile strength, elongation at break and young modulus of the polymer films

Sample type	Tensile Strength (MPa)	Elongation at Break (%)	Young Modulus (GPa)
CS-PVA	49.72 ± 12.01	1.65 ± 1.45	3.88 ± 0.09
CS-1V-PVA	59.12 ± 3.98	1.53 ± 0.14	4.29 ± 0.24
CS-3V-PVA	63.8 ± 8.76	1.47 ± 0.49	5.16 ± 0.55

Ninhydrin assay is an indirect method for quantification of the remaining free amino groups and calculation of the crosslinking degree in the blended films. The reaction between the free amino groups of CS and ninhydrin reagent forms chitosan-ninhydrin complexes which have a purple color known as Ruhemann's purple and a decrease in the ninhydrin chromophore is directly related to the extent of crosslinking. As seen in Figure 9, the color lightens with the increase in vanillin concentration which indicates a decrease in the number of free amino groups. The crosslinking degree of CS-PVA blend films is 26.3 ± 3.25%. This result could be attributed to the formation intermolecular hydrogen bonds between amino and hydroxyl groups of CS and hydroxyl groups of PVA [65,66]. The highest degree of crosslinking is achieved when the amount of vanillin is 3 % (74.4 ± 2.5%), confirming the Schiff base reaction between amino groups of CS and aldehyde group of vanillin. In case of CS-1V-PVA films, the decrease in the vanillin concentration slightly decreases the crosslinking degree to 69.3 ± 2.9%. The crosslinking degrees obtained in the present work are similar to those reported. Abraham et al. [21] synthesized microwave assisted crosslinked CS with 66% crosslinking degree for 1% vanillin concentration and Jagadish et al [67] reported a 63% crosslinking for vanillin modified CS with sodium cyanoborohydride reduction.

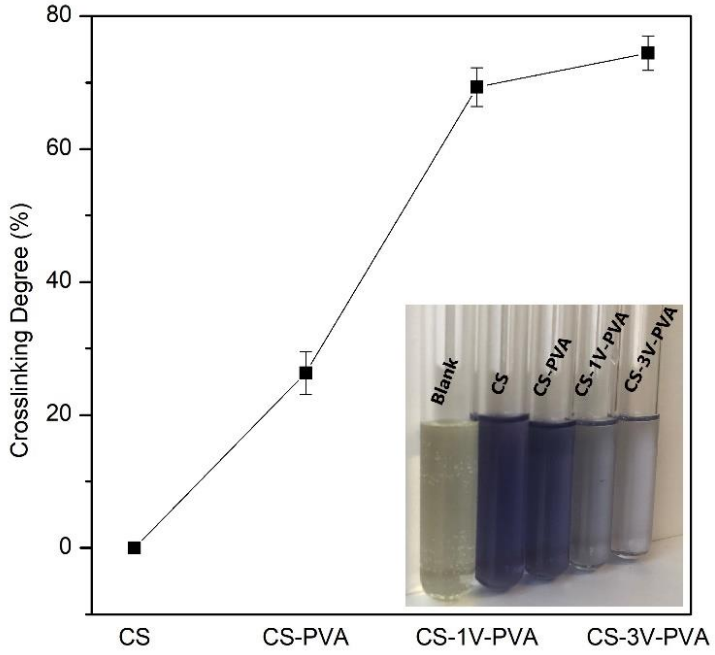

Figure 9. Crosslinking degree of CS-PVA films and the color of the sample–ninhydrin complex (inset image)

3.2. Swelling Measurement

In transdermal systems, the capacity of swelling plays a significant role for loading and release behavior of the drug [68]. An optimum degree of swelling is necessary since the low swelling forms a weak bioadhesive strength whereas high swelling causes a burst drug release that affects the delivery efficiency [69]. The obtaining of this optimum level of swelling is directly related to the type of polymers incorporated in the blend as well as the crosslinking agents.

Table 2 shows the degree of swelling for the raw CS film and all the blend except drug-loaded counterparts. All preparations show a swelling degree that ranges from 319.3% to 36.3% with significant difference ($p < 0.05$). The highest swelling capacity is exhibited by the raw CS film which has hydrophilic groups on the polymer backbone to form hydrogen bonds with water. The swelling degree obtained for CS-PVA blend is 243.7% which is distinctly lower than the obtained for raw CS film. This reduction in swelling volume could be attributed to the decrease in the number of hydrophilic groups in the blend due to the interactions between the functional groups of CS and PVA [70]. It can be also concluded from the table that varying vanillin concentration has a strong influence on the

swelling capacity by decreasing it from 243.7% to 36.3%. As the material crosslinked with vanillin, the CS-PVA matrix interactions increase and a more rigid network forms by the inter and intra-polymer reactions; hence the water penetration into polymer blend structure is restricted by these new interactions. As expected, equilibrium water contents of the vanillin crosslinked films exhibit a decreasing tendency with increasing vanillin content due to CS amine groups being more reactive to vanillin than to hydroxyls of PVA. This result is in agreement with previous studies [71,72] which reported that crosslinker decreases the swelling degree due to acetylation and the formation of the Schiff base [73] between the CS and vanillin molecules that restricts the penetration of water molecules. According to reported literature, such moderate percent swelling is regarded as sufficient for proper adhesion and *in vitro* drug release [74].

3.4. In-vitro Drug Release Test

The *in vitro* release profiles of ENR from CS-PVA films are presented in Figure 10, in terms of cumulative release versus time. In the release profiles, two-step process based on a slight initial burst release and following subsequent slower release is beneficial as it helps to achieve the therapeutic drug concentration for blocking of biofilm formation in the first place and then maintaining a sustained and controlled release [37]. In the initial burst release phase, ENR molecules absorbed and entrapped near the surface were released due to the high dissolution rate of the polymer near the surface. For the non-crosslinked CS-PVA blend, the ENR was rapidly released and its cumulative release reached to 50% in 3h. However, the release rate was significantly reduced to 15-25% by the crosslinking reaction of CS with vanillin. The subsequent slower release from vanillin crosslinked films accounted for the effect of vanillin on limiting access of water and dissolution of the drug. Figure 10 showed that with the increase in vanillin content, the 3% vanillin crosslinked film yielded the lowest cumulative percentages of drug release in 12h. Besides the crosslinking, this can be also explained by the hydrophobicity of the drug delivery system which also has impact on controlling the release. Here, the hydrophobic interactions of vanillin crosslinked blend films were increased with the vanillin concentration and led to a retarded release of drug from the polymer matrix [75,76].

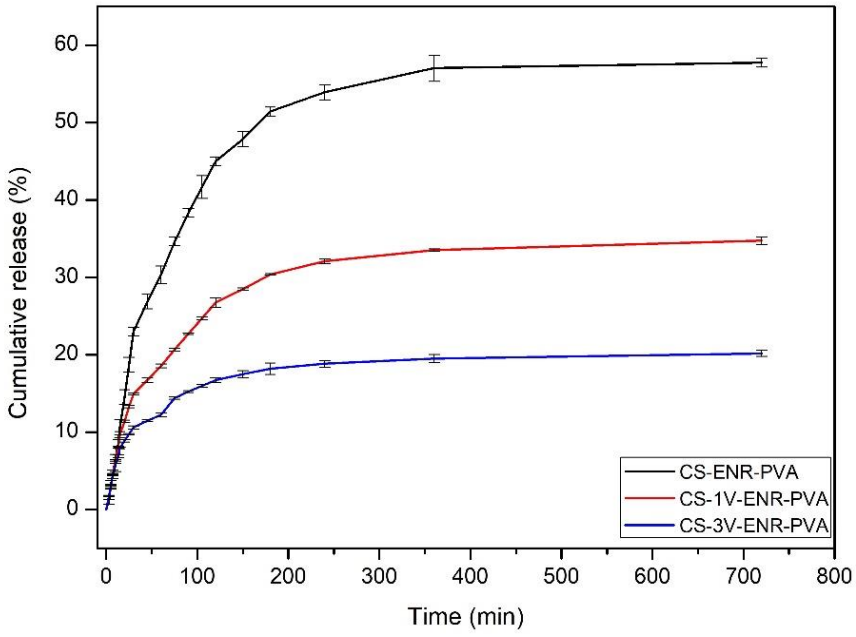

Figure 10. *In-vitro* drug release profiles of ENR-loaded CS-PVA films

The calculated drug loading efficiency of the non-crosslinked film in the PBS medium was rather lower than those vanillin crosslinked ones (Table 5). The ENR content for 3% vanillin crosslinked film was found the highest of drug content with 94.8%, which is also coincided with XPS results. When the vanillin concentration decreases from 3% to 1%, the ENR loading also decreases significantly to 59.9%. This drug loading behavior is attributed to the higher crosslinker concentration which mediates the higher Schiff Base reaction between the amino groups of CS and aldehyde group of vanillin that

increase the retention of drug molecules. In comparison, the release rate of ENR followed the descending order: CS-ENR-PVA > CS-1V-ENR-PVA > CS-3V-ENR-PVA.

Table 5. Effect of vanillin concentration on the release kinetics

Formulation	Drug Loading Efficiency (%)	Zero order	First order	Higuchi	Korsmeyer-Peppas	
		R^2	R^2	R^2	R^2	n
CS-ENR-PVA	49.1	0.924	0.960	0.982	0.898	0.63
CS-1V-ENR-PVA	59.9	0.896	0.922	0.984	0.943	0.52
CS-3V-ENR-PVA	94.8	0.832	0.851	0.964	0.977	0.41

The mechanism of drug release for studied formulations was investigated using various kinetic models and the results were presented in Table 5. The best fit for the highest value of the regression coefficient (R^2) provides the release model. The regression coefficient value for all the ENR-loaded films is found to be the highest for the Higuchi model which implies that the release mechanism is controlled by diffusion and erosion (dissolution) forces. Once the mechanism follows the Higuchi model, further confirmation of the release profile is investigated by the Korsmeyer-Peppas model to explain the diffusion type from the polymer matrix [77]. In this model, the diffusion mechanism from the polymer matrix is commanded by the exponent value 'n'. This value indicates that the diffusion mechanism is Fickian, anomalous transport, or super case II transport [78]. Herein, the 'n' values decrease with the increase in vanillin concentration. The mechanism for the non-crosslinked and 1% vanillin crosslinked film was governed anomalous transport ($0.45 < n < 0.89$) which indicates that the release tends to be controlled by swelling and polymer relaxation. This result also coincides with the swelling degrees of these two films which have higher swelling values than the 3% vanillin crosslinked film. The value of $n \leq 0.45$ for 3% vanillin crosslinked film suggested that the drug release mechanism closely fitted Fickian diffusion which also showed that this approach helped reduce the initial burst release. Furthermore, the reduced release rate of the ENR from the 3% vanillin crosslinked film correlated to its lower swelling degree as reported in previous studies. [69,79].

4. Conclusions

The matrix-type transdermal film systems based on CS and PVA were successfully prepared through a simple and easily reproducible solvent-casting method without using any penetration enhancer and plasticizer. The only addition to the polymer blend was vanillin as a crosslinker that was chosen for its natural origin. The vanillin crosslinked film formation was confirmed by FTIR and ninhydrin assay. The survey scan XPS spectra demonstrated that the increase in the vanillin concentration resulted in increased drug loading efficiency. Furthermore, SEM images showed that the presence of vanillin reduced the risk of drug agglomeration and provided uniform distribution of the ENR in the blend films. To verify this phenomenon, the topography of films with/without vanillin was investigated by AFM analysis and the images demonstrated that the surface roughness of vanillin incorporated film is lower as a result of crosslinking. The investigations on the mechanical properties indicated that tensile properties were increased considerably by vanillin addition, the film being stiffer than non-crosslinked films. The optimum swelling degree of the prepared films mainly originated from the vanillin presence that led to the construction of the Schiff-base bond. As a result, the restricted movement of polymer molecule chains in a compact network presented a sustained drug release behavior. It was found that ENR release was influenced by the amount of vanillin incorporated within the CS-PVA blend, especially, adding amount 3%. These findings will pave the way for a future study to characterize important parameters, such as pH, concentration and temperature and also for *in vivo* studies. Overall, all these results suggest that the proposed material with higher crosslink density can be used as an ideal matrix with enhanced release kinetics for potential local drug delivery applications.

Acknowledgements: Authors thank the Internal Grant Agency of Tomas Bata University in Zlín (IGA/CPS/2021/001), the Ministry of Education, Youth, and Sports of the Czech Republic (project no. LTACH17015) and NPU Program I (LO1504) for financial support.

Conflicts of Interest: The authors declare no conflict of interest.

References

1. Sachan, R., Bajpai, M. Transdermal drug delivery system: A Review. Int. J. Res. Dev. Pharm. L. Sci., **2013**, 3(1), pp. 748-765. doi: 10.21276/IJRDPL
2. Marwah, H., Garg, T., Goyal, A. K., Rath, G. Permeation enhancer strategies in transdermal drug delivery. Drug Delivery, **2014**, 23(2), 564–578. doi: 10.3109/10717544.2014.935532
3. Mehtani, D., Seth, A., Sharma, P., Maheshwari, N., Kapoor, D., Shrivastava, S. K., Tekade, R. K. Biomaterials for Sustained and Controlled Delivery of Small Drug Molecules. Biomaterials and Bionanotechnology, **2019**, 89-152. doi:10.1016/b978-0-12-814427-5.00004-4
4. Saikia, C., Gogoi, P. Chitosan: A Promising Biopolymer in Drug Delivery Applications. Journal of Molecular and Genetic Medicine, **2015**, S4. doi:10.4172/1747-0862.s4-006
5. Bayat, M., Nasri, S. Injectable microgel–hydrogel composites "plum pudding gels": New system for prolonged drug delivery. Nanomaterials for Drug Delivery and Therapy, **2019**, 343-372. doi:10.1016/b978-0-12-816505-8.00001-1
6. Karkossa, F., Klein, S. Individualized in vitro and in silico methods for predicting in vivo performance of enteric-coated tablets containing a narrow therapeutic index drug. European Journal of Pharmaceutics and Biopharmaceutics, **2019**, 135, 13-24 doi:10.1016/j.ejpb.2018.12.004
7. Siddaramaiah, K. P., Divya K. H., Mhemavathi B. T., Manjula D. S. Chitosan/HPMC Polymer Blends for Developing Transdermal Drug Delivery Systems. Journal of Macromolecular Science, **2006**, Part A: Pure and Applied Chemistry, 43(3), 601-607. doi:10.1080/10601320600575231
8. Basavaraj, K. H., Johnsy, G., Navya, M. N., Rashmi, R., Siddaramaiah. Biopolymers as Transdermal Drug Delivery Systems in Dermatology Therapy. *Critical Reviews in Therapeutic Drug Carrier Systems*, **2010**, vol. 27, no. 2, pp. 155–185. doi:10.1615/critrevtherdrugcarriersyst.v27.i2.20.
9. Arriagada, F., Morales, J. Limitations and Opportunities in Topical Drug Delivery: Interaction Between Silica Nanoparticles and Skin Barrier. Current Pharmaceutical Design, **2019**, 25(4), 455-466. doi:10.2174/1381612825666190404121507
10. Shaker, D. S., Ishak, R. A., Ghoneim, A., Elhuoni, M. A. Nanoemulsion: A Review on Mechanisms for the Transdermal Delivery of Hydrophobic and Hydrophilic Drugs. Scientia Pharmaceutica, **2019,** 87(3), 17. doi:10.3390/scipharm87030017
11. Muzzalupo, R., Tavano, L. Niosomal drug delivery for transdermal targeting: Recent advances. Research and Reports in Transdermal Drug Delivery, **2015**, 23. doi:10.2147/rrtd.s64773
12. Liu, H., Wang, C., Li, C., Qin, Y., Wang, Z., Yang, F., Wang, J., et al. A functional chitosan-based hydrogel as a wound dressing and drug delivery system in the treatment of wound healing. RSC Advances, **2018**, 8(14), 7533–7549. doi: 10.1039/c7ra13510f
13. Nawaz, A., Khan, N., Vigneswaran, T. Chitosan and Its Roles in Transdermal Drug Delivery. Handbook of Sustainable Polymers, **2015**, 557–586. doi: 10.1201/b19600-17
14. Barclay, T. G., Day, C. M., Petrovsky, N., Garg, S. Review of polysaccharide particle-based functional drug delivery. Carbohydrate Polymers, **2019**, 221, 94-112. doi:10.1016/j.carbpol.2019.05.067
15. Gao, H.-X., He, Z., Sun, Q., He, Q., Zeng, W.C. A functional polysaccharide film forming by pectin, chitosan, and tea polyphenols. Carbohydrate Polymers, **2019**, 215, 1–7. doi: 10.1016/j.carbpol.2019.03.029
16. Ozaltin, K., Postnikov, P. S., Trusova, M. E., Sedlarik, V., & Martino, A. D. Polysaccharides based microspheres for multiple encapsulations and simultaneous release of proteases. International Journal of Biological Macromolecules, **2019**, 132, 24–31. doi: 10.1016/j.ijbiomac.2019.03.189
17. Long, J., Etxeberria, A. E., Nand, A. V., Bunt, C. R., Ray, S., Seyfoddin, A. (2019). A 3D printed chitosan-pectin hydrogel wound dressing for lidocaine hydrochloride delivery. Materials Science and Engineering: C, 104, 109873. doi: 10.1016/j.msec.2019.109873

18. Govindaraj, P., Abathodharanan, N., Ravishankar, K., Raghavachari, D. Facile preparation of biocompatible macroporous chitosan hydrogel by hydrothermal reaction of a mixture of chitosan-succinic acid-urea. Materials Science and Engineering: C, **2019**, 104, 109845. doi: 10.1016/j.msec.2019.109845
19. Bellich, B., D'Agostino, I., Semeraro, S., Gamini, A., Cesàro, A. "The Good, the Bad and the Ugly" of Chitosans. Marine Drugs, **2016**, 14(5), 99. doi: 10.3390/md14050099
20. He, W., Guo, X., Xiao, L., Feng, M. Study on the mechanisms of chitosan and its derivatives used as transdermal penetration enhancers. International Journal of Pharmaceutics, **2009**, 382(1-2), 234-243. doi:10.1016/j.ijpharm.2009.07.038
21. Abraham, S., Rajamanick, D., Srinivasan, B. Preparation, Characterization and Cross-linking of Chitosan by Microwave Assisted Synthesis. Science International, **2018**, 6(1), 18–30. doi: 10.17311/sciintl.2018.18.30
22. Walke, S., Srivastava, G., Nikalje, M., Doshi, J., Kumar, R., Ravetkar, S., Doshi, P. Fabrication of chitosan microspheres using vanillin/TPP dual crosslinkers for protein antigens encapsulation. Carbohydrate Polymers, **2015**, 128, 188–198. doi:10.1016/j.carbpol.2015.04.020
23. Wang, L., Guo, H., Wang, J., Jiang, G., Du, F., Liu, X. Effects of Herba Lophatheri extract on the physicochemical properties and biological activities of the chitosan film. International Journal of Biological Macromolecules, **2019**, 133, 51–57. doi: 10.1016/j.ijbiomac.2019.04.067
24. Chen, C., Liu, L., Huang, T., Wang, Q., Fang, Y. E. Bubble template fabrication of chitosan/poly(vinyl alcohol) sponges for wound dressing applications. International Journal of Biological Macromolecules, **2013**, 62, 188–193. doi: 10.1016/j.ijbiomac.2013.08.042
25. Bhumkar, D. R., Pokharkar, V. B. Studies on effect of pH on cross-linking of chitosan with sodium tripolyphosphate: A technical note. AAPS PharmSciTech, **2006**, 7(2). doi: 10.1208/pt070250
26. Zhang, Z.-H., Han, Z., Zeng, X.-A., Xiong, X.-Y., Liu, Y.-J. Enhancing mechanical properties of chitosan films via modification with vanillin. International Journal of Biological Macromolecules, **2015**, 81, 638–643. doi: 10.1016/j.ijbiomac.2015.08.042
27. Zhou, G., A., R., Ge, H., Wang, L., Liu, M., Wang, B., Fan, Y., et al. Research on a novel poly (vinyl alcohol)/lysine/vanillin wound dressing: Biocompatibility, bioactivity and antimicrobial activity. Burns, **2014**, 40(8), 1668–1678. doi: 10.1016/j.burns.2014.04.005
28. Jimtaisong, A., & Saewan, N. Plant-Derived Polyphenols as Potential Cross-Linking Agents for Methylcellulose-Chitosan Biocomposites. Solid State Phenomena, **2018**, 283, 140-146. doi:10.4028/www.scientific.net/ssp.283.140
29. Dalmolin, L. F., Khalil, N. M., Mainardes, R. M. Delivery of vanillin by poly(lactic-acid) nanoparticles: Development, characterization and in vitro evaluation of antioxidant activity. Materials Science and Engineering: C, **2016**, 62, 1–8. doi: 10.1016/j.msec.2016.01.031
30. Kamaraj, S., Palanisamy, U. M., Mohamed, M. S. B. K., Gangasalam, A., Maria, G. A., Kandasamy, R. Curcumin drug delivery by vanillin-chitosan coated with calcium ferrite hybrid nanoparticles as carrier. European Journal of Pharmaceutical Sciences, **2018**, 116, 48–60. doi: 10.1016/j.ejps.2018.01.023
31. Xu, C., Zhan, W., Tang, X., Mo, F., Fu, L., Lin, B. Self-healing chitosan/vanillin hydrogels based on Schiff-base bond/hydrogen bond hybrid linkages. Polymer Testing, **2018**, 66, 155–163. doi: 10.1016/j.polymertesting.2018.01.016
32. Zou, Q., Li, J., Li, Y. Preparation and characterization of vanillin-crosslinked chitosan therapeutic bioactive microcarriers. International Journal of Biological Macromolecules, **2015**, 79, 736–747. doi: 10.1016/j.ijbiomac.2015.05.037
33. Kasai, D., Chougale, R., Masti, S., Narasgoudar, S. Thermal degradation of ternary blend films containing PVA/chitosan/vanillin. **2018** doi: 10.1063/1.5032561
34. Baghel, S., Cathcart, H., Oreilly, N. J. ChemInform Abstract: Polymeric Amorphous Solid Dispersions: A Review of Amorphization, Crystallization, Stabilization, Solid-State Characterization, and Aqueous Solubilization of Biopharmaceutical Classification System Class II Drugs. ChemInform, **2016**, 47(42). doi: 10.1002/chin.201642262

35. Sahoo, A., Kumar, N. K., Suryanarayanan, R. Crosslinking: An avenue to develop stable amorphous solid dispersion with high drug loading and tailored physical stability. Journal of Controlled Release, **2019**, 311-312, 212–224. doi: 10.1016/j.jconrel.2019.09.007
36. Wang, H., Qian, J., Ding, F. Emerging Chitosan-Based Films for Food Packaging Applications. Journal of Agricultural and Food Chemistry, **2018**, 66 (2), 395-413 doi: 10.1021/acs.jafc.7b04528
37. Peng, H., Xiong, H., Li, J., Xie, M., Liu, Y., Bai, C., Chen, L. Vanillin cross-linked chitosan microspheres for controlled release of resveratrol. Food Chemistry, **2010**, 121(1), 23–28. doi: 10.1016/j.foodchem.2009.11.085
38. Li, P.-W., Wang, G., Yang, Z.-M., Duan, W., Peng, Z., Kong, L.-X., Wang, Q.-H. Development of drug-loaded chitosan–vanillin nanoparticles and its cytotoxicity against HT-29 cells. Drug Delivery, **2014**, 23(1), 30–35. doi: 10.3109/10717544.2014.900590
39. Sangalli, M., Zema, L., Maroni, A., Foppoli, A., Giordano, F., Gazzaniga, A. Influence of betacyclodextrin on the release of poorly soluble drugs from inert and hydrophilic heterogeneous polymeric matrices. Biomaterials, **2001**, 22(19), 2647-2651. doi:10.1016/s0142-9612(01)00005-9
40. Parikh, T., Gupta, S. S., Meena, A. K., Vitez, I., Mahajan, N., Serajuddin, A. T. Application of Film-Casting Technique to Investigate Drug–Polymer Miscibility in Solid Dispersion and Hot-Melt Extrudate. Journal of Pharmaceutical Sciences, **2015**, 104(7), 2142-2152. doi:10.1002/jps.24446
41. Qian, F., Huang, J., Hussain, M. A. Drug–Polymer Solubility and Miscibility: Stability Consideration and Practical Challenges in Amorphous Solid Dispersion Development. Journal of Pharmaceutical Sciences, **2010**, 99(7), 2941-2947. doi:10.1002/jps.22074
42. Zhang, X., Xing, H., Zhao, Y., Ma, Z. Pharmaceutical Dispersion Techniques for Dissolution and Bioavailability Enhancement of Poorly Water-Soluble Drugs. Pharmaceutics, **2018**, 10(3), 74. doi:10.3390/pharmaceutics10030074
43. Shi, X., Huang, W., Xu, T., Fan, B., Sheng, X. Investigation of Drug–Polymer Miscibility and Solubilization on Meloxicam Binary Solid Dispersion. Journal of Pharmaceutical Innovation, 2019, 15(1), 125-137. doi:10.1007/s12247-019-09378-4
44. Ma, L. The investigation of Fluorescence spectra and Fluorescence quantum yield of Enrofloxacin. Journal of Chemical, Environmental and Biological Engineering, **2018**, 2(1), 11. doi:10.11648/j.jcebe.20180201.13
45. Vargun, E., Ozaltin, K., Fei, H., Harea, E., Vilčáková, J., Kazantseva, N., Saha, P. Biodegradable porous polylactic acid film as a separator for supercapacitors. Journal of Applied Polymer Science, **2020**, 137(42), 49270. doi:10.1002/app.49270
46. Cui, L., Jia, J., Guo, Y., Liu, Y., & Zhu, P. Preparation and characterization of Ipn Hydrogels composed of chitosan and Gelatin Cross-linked by Genipin. Carbohydrate Polymers, **2014**, 99, 31-38. doi:10.1016/j.carbpol.2013.08.048
47. Marin, L., Stoica, I., Mares, M., Dinu, V., Simionescu, B. C., Barboiu, M. Antifungal vanillin–imino-chitosan biodynameric films. Journal of Materials Chemistry B, **2013**, 1(27), 3353. doi: 10.1039/c3tb20558d
48. Aryaei, A., Jayatissa, A. H., Jayasuriya, A.C. Nano and micro mechanical properties of uncross-linked and cross-linked chitosan films. Journal of the Mechanical Behavior of Biomedical Materials, **2012**, 5(1), 82-89. doi:10.1016/j.jmbbm.2011.08.006
49. Karakeçili, A. G., Satriano, C., Gümüşderelioğlu, M., Marletta, G. Surface characteristics of ionically crosslinked chitosan membranes. Journal of Applied Polymer Science, **2007**, 106(6), 3884-3888. doi:10.1002/app.26920
50. Wen, H., & Park, K. Oral controlled release formulation design and drug delivery: theory to practice. Hoboken, NJ: Wiley, **2010**, pp. 139-146. doi: 10.1002/9780470640487
51. Chen, Y., Lam, J. W., Kwok, R. T., Liu, B., Tang, B. Z. Aggregation-induced emission: Fundamental understanding and future developments. Materials Horizons, **2019**, 6(3), 428-433. doi:10.1039/c8mh01331d

52. Mansur, H. S., Sadahira, C. M., Souza, A. N., Mansur, A. A. FTIR spectroscopy characterization of poly (vinyl alcohol) hydrogel with different hydrolysis degree and chemically crosslinked with glutaraldehyde. Materials Science and Engineering: C, **2008**, 28(4), 539–548. doi: 10.1016/j.msec.2007.10.088
53. Pawlak, A., Mucha, M. Thermogravimetric and FTIR studies of chitosan blends. Thermochimica Acta, **2003**, 396(1-2), 153–166. doi: 10.1016/s0040-6031(02)00523-3
54. Cardenas, G., Miranda, S. P. Ftir And Tga Studies Of Chitosan Composite Films. Journal of the Chilean Chemical Society, **2004**, 49(4). doi: 10.4067/s0717-97072004000400005
55. Wang, G., Li, P. W., Peng, Z., Huang, M. F., Kong, L. X. Formulation of Vanillin Cross-Linked Chitosan Nanoparticles and its Characterization. Advanced Materials Research, **2011**, 335-336, 474–477. doi: 10.4028/www.scientific.net/amr.335-336.474
56. Shekarforoush, E., Mendes, A., Baj, V., Beeren, S., Chronakis, I. Electrospun Phospholipid Fibers as Micro-Encapsulation and Antioxidant Matrices. Molecules, **2017**, 22(10), 1708. doi: 10.3390/molecules22101708
57. Srithongkham, S., Sutcharee, P., Lertworasirikul, A. Investigation of Synthesis Parameters for Modification of Chitosan with Enrofloxacin. Key Engineering Materials, **2015**, 659, 436–440. doi: 10.4028/www.scientific.net/kem.659.436
58. Kumar, G. P., Phani, A., Prasad, R., Sanganal, J. S., Manali, N., Gupta, R., Raju, D., et al. Polyvinylpyrrolidone oral films of enrofloxacin: Film characterization and drug release. International Journal of Pharmaceutics, **2014**, 471(1-2), 146–152. doi:10.1016/j.ijpharm.2014.05.033
59. Martinez, Y. N., Piñuel, L., Castro, G. R., & Breccia, J. D. Polyvinyl Alcohol–Pectin Cryogel Films for Controlled Release of Enrofloxacin. Applied Biochemistry and Biotechnology, **2012**, 167(5), 1421–1429. doi: 10.1007/s12010-012-9554-6
60. Alves, N. O., Silva, G. T. D., Weber, D. M., Luchese, C., Wilhelm, E. A., Fajardo, A. R. Chitosan/poly(vinyl alcohol)/bovine bone powder biocomposites: A potential biomaterial for the treatment of atopic dermatitis-like skin lesions. Carbohydrate Polymers, **2016**, 148, 115–124. doi: 10.1016/j.carbpol.2016.04.049
61. Casey, L. S., & Wilson, L. D. Investigation of Chitosan-PVA Composite Films and Their Adsorption Properties. Journal of Geoscience and Environment Protection, **2015**, 03(02), 78–84. doi: 10.4236/gep.2015.32013
62. Wu, H., Lei, Y., Lu, J., Zhu, R., Xiao, D., Jiao, C., Li, M. Effect of citric acid induced crosslinking on the structure and properties of potato starch/chitosan composite films. Food Hydrocolloids, **2019**, 97, 105208. doi:10.1016/j.foodhyd.2019.105208
63. Wahba, M. I. Enhancement of the mechanical properties of chitosan. Journal of Biomaterials Science, Polymer Edition, **2019**, 31(3), 350-375. doi:10.1080/09205063.2019.1692641
64. Narasagoudr, S. S., Hegde, V. G., Vanjeri, V. N., Chougale, R. B., Masti, S. P. Ethyl vanillin incorporated chitosan/poly(vinyl alcohol) active films for food packaging applications. Carbohydrate Polymers, **2020**, 236, 116049. doi:10.1016/j.carbpol.2020.116049
65. Koosha, M., Hamedi, S. Intelligent Chitosan/PVA nanocomposite films containing black CARROT anthocyanin and bentonite nanoclays with improved mechanical, thermal and antibacterial properties. Progress in Organic Coatings, **2019**, 127, 338-347. doi:10.1016/j.porgcoat.2018.11.028
66. Olewnik-Kruszkowska, E., Gierszewska, M., Jakubowska, E., Tarach, I., Sedlarik, V., Pummerova, M. Antibacterial films based on PVA and PVA–Chitosan modified With Poly(Hexamethylene Guanidine). Polymers, **2019**, 11(12), 2093. doi:10.3390/polym11122093
67. Jagadish, R., Divyashree, K., Viswanath, P., Srinivas, P., Raj, B. Preparation of n-vanillyl chitosan and 4-hydroxybenzyl chitosan and their physico-mechanical, optical, barrier, and antimicrobial properties. Carbohydrate Polymers, **2012**, 87(1), 110-116. doi:10.1016/j.carbpol.2011.07.024
68. Kumria, R., Nair, A. B., Goomber, G., Gupta, S. Buccal films of prednisolone with enhanced bioavailability. Drug Delivery, **2014**, 23(2), 471–478. doi: 10.3109/10717544.2014.920058

69. Enin, H. A. A., Nabarawy, N. A. E., Elmonem, R. A. A. Treatment of Radiation-Induced Oral Mucositis Using a Novel Accepted Taste of Prolonged Release Mucoadhesive Bi-medicated Double-Layer Buccal Films. AAPS PharmSciTech, **2016**, 18(2), 563–575. doi:10.1208/s12249-016-0533-z
70. Mozafari, M., Moztarzadeh, Jalali, Alhosseini, N., Asgari, Dodel, Kargozar., et al. Synthesis and characterization of electrospun polyvinyl alcohol nanofibrous scaffolds modified by blending with chitosan for neural tissue engineering. International Journal of Nanomedicine, **2012**, 25. doi: 10.2147/ijn.s25376
71. Stroescu, M., Stoica-Guzun, A., Jipa, I. M. Vanillin release from poly(vinyl alcohol)-bacterial cellulose mono and multilayer films. Journal of Food Engineering, **2013**, 114(2), 153–157. doi: 10.1016/j.jfoodeng.2012.08.023
72. Vimala, K., Mohan, Y. M., Sivudu, K. S., Varaprasad, K., Ravindra, S., Reddy, N. N., Mohanaraju, K., et al. Fabrication of porous chitosan films impregnated with silver nanoparticles: A facile approach for superior antibacterial application. Colloids and Surfaces B: Biointerfaces, **2010**, 76(1), 248–258. doi: 10.1016/j.colsurfb.2009.10.044
73. Bernal-Ballen, A., Lopez-Garcia, J.-A., Ozaltin, K. (PVA/Chitosan/Fucoidan)-Ampicillin: A Bioartificial Polymeric Material with Combined Properties in Cell Regeneration and Potential Antibacterial Features. Polymers, **2019**, 11(8), 1325. doi: 10.3390/polym11081325
74. Al-Dhubiab, B. E., Nair, A. B., Kumria, R., Attimarad, M., Harsha, S. Development and evaluation of buccal films impregnated with selegiline-loaded nanospheres. Drug Delivery, **2014**, 1–9. doi: 10.3109/10717544.2014.948644
75. Cui, Z., Zheng, Z., Lin, L., Si, J., Wang, Q., Peng, X., Chen, W. Electrospinning and crosslinking of polyvinyl alcohol/chitosan composite nanofiber for transdermal drug delivery. Advances in Polymer Technology, **2017**, 37(6), 1917–1928. doi: 10.1002/adv.21850
76. Al-Kassas, R., Wen, J., Cheng, A. E.-M., Kim, A. M.-J., Liu, S. S. M., Yu, J. Transdermal delivery of propranolol hydrochloride through chitosan nanoparticles dispersed in mucoadhesive gel. Carbohydrate Polymers, **2016**, 153, 176–186. doi:10.1016/j.carbpol.2016.06.096
77. Mathematical models of drug release. (2015). Strategies to Modify the Drug Release from Pharmaceutical Systems, 63–86. doi: 10.1016/b978-0-08-100092-2.00005-9
78. Motiei, M., Sedlařík, V., Lucia, L. A., Fei, H., Münster, L. Stabilization of chitosan-based polyelectrolyte nanoparticle cargo delivery biomaterials by a multiple ionic cross-linking strategy. Carbohydrate Polymers, 2020, 231, 115709. doi: 10.1016/j.carbpol.2019.115709
79. Hezaveh, H., & Muhamad, I. I. Controlled drug release via minimization of burst release in pH-response kappa-carrageenan/polyvinyl alcohol hydrogels. Chemical Engineering Research and Design, **2013**, 91(3), 508–519. doi: 10.1016/j.cherd.2012.08.014